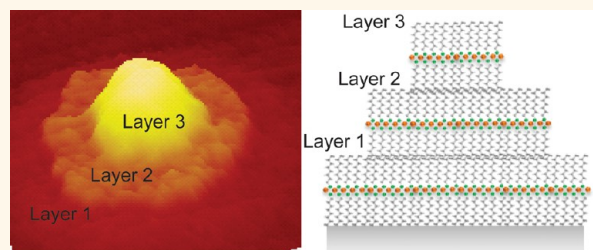


Layer-by-Layer Assembly of a Metallomesogen by Dip-Pen Nanolithography

Boya Radha,[†] Guoliang Liu,[‡] Daniel J. Eichelsdoerfer,[‡] Giridhar U. Kulkarni,[§] and Chad A. Mirkin^{†,‡,*}

[†]Department of Materials Science and Engineering and [‡]Department of Chemistry and International Institute for Nanotechnology, Northwestern University, 2145 Sheridan Road, Evanston, Illinois 60208, United States and [§]Chemistry and Physics of Materials Unit and DST Unit on Nanoscience, Jawaharlal Nehru Centre for Advanced Scientific Research, Jakkur P.O., Bangalore 560 064, India

ABSTRACT Palladium alkanethiolates are introduced here as a novel liquid ink for dip-pen nanolithography (DPN). These structures exhibit the unusual characteristic of layer-by-layer assembly, allowing one to deposit a desired number of metal ions on a surface, which can subsequently be reduced *via* thermolysis to form active catalytic structures. Such structures have been used to generate contiguous metallic or conducting polymer nanoscale architectures by electroless deposition.



KEYWORDS: dip-pen nanolithography · lamellar assembly · molecular printing · metal alkanethiolate · scanning probe lithography

Dip-pen nanolithography (DPN)¹ is a direct-write lithography technique that utilizes atomic force microscope (AFM) tips coated with molecular inks in order to precisely deliver molecules to a substrate.^{2,3} In the early stages of DPN development, researchers relied on alkanethiols as inks since they readily form self-assembled monolayers (SAMs) on Au.⁴ In recent years, the DPN tool-kit has rapidly expanded to other inks, including polymers,⁵ proteins,⁶ DNA,⁷ metal ions,⁸ nanoparticles,⁹ sols,¹⁰ liquid-crystalline inks such as collagen,¹¹ and phospholipids.¹² Traditionally, DPN has been used for three different applications: (1) patterning chemical adlayers on surfaces in order to create patterns on the underlying substrate, (2) patterning “soft” materials such as chemical and biological molecules, and (3) patterning molecular precursors to convert them into hard materials by post-processing methods. For all of these applications, the strength of DPN lies in the ease of writing structures that are one molecule thick. This strength, however, can also be a limitation, as there is currently no method for controlling the number of layers in a deposited feature. Monolayers and well-controlled multilayers of molecules have generated immense research interest since

they represent ideal 2-D model systems for studying the evolution of materials with interesting physical and chemical phenomena at surfaces/interfaces.¹³ While one can build up layer-by-layer atomic structures by sophisticated epitaxial growth,¹⁴ incorporating metal ions between organic monolayers is an alternative method for building similar molecular structures.¹⁵ A popular technique for depositing organic monolayers is Langmuir–Blodgett assembly,¹⁶ which makes molecular thin films with controlled height but cannot be used to fabricate laterally confined nanoscale structures without post-lithography processes.¹⁷ Another technique, termed constructive lithography,¹⁸ makes use of a conducting AFM tip for modifying the terminal functional groups on molecular layers for subsequent templating.^{19,20} Here, we explore how metal alkanethiolates (Figure 1) can be used as novel DPN inks to form three-dimensional features in a direct-write layer-by-layer fashion. Metal alkanethiolates were chosen as a prototypical ink for forming three-dimensional structures because they readily self-assemble into multilayer structures that resemble phospholipid bilayer structures.¹² Moreover, these molecules possess electrical and magnetic properties

* Address correspondence to chadnano@northwestern.edu.

Received for review December 28, 2012 and accepted February 5, 2013.

Published online February 12, 2013
10.1021/nn306013e

© 2013 American Chemical Society

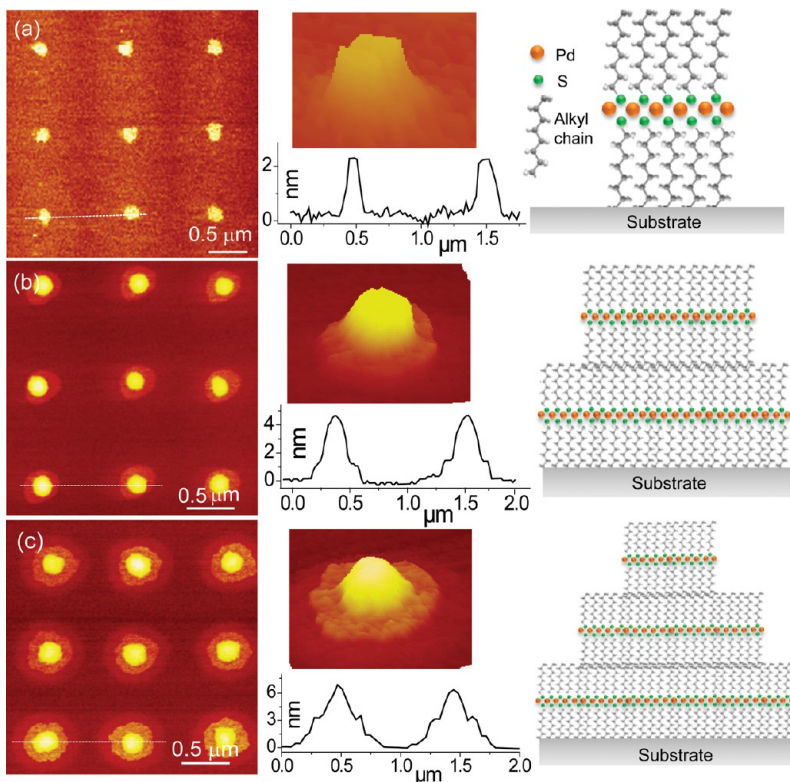


Figure 1. Site-specific deposition of Pd octylthiolate lamellar layers: AFM topography images of (a) a single molecular layer, (b) two layers, and (c) three layers with z-profiles. The schematic arrangement of Pd octylthiolate lamellae is shown alongside.

that are of potential technological importance, such as negative differential resistance²¹ and antiferromagnetic coupling.²²

While various metal thiolates, including those made from Au,²³ Ag,²⁴ Cu,²⁵ and Ni,¹⁹ have been studied extensively in their bulk form, there is little work on metal alkanethiolate SAMs due to the difficulty in transferring them homogeneously to surfaces.²⁴ While some researchers have used conventional lithography techniques such as e-beam lithography to create patterns of metal alkanethiolates on surfaces in a site-specific manner,²⁶ the deposition of these molecules in their intact form, with precise control over both the height and feature size, cannot be done. Herein, we show how DPN and dilute solutions of metal alkanethiolates as inks can be used to generate surface structures with control over feature size, height, and resolution. Surprisingly, one can control the deposition of metal alkanethiolate structures with nanoscale resolution, one layer at a time. This capability will be useful for creating nanoscale reactors²⁰ where the number of metal ions in a structure can be precisely controlled by the three-dimensional architecture generated in the DPN experiment. As a proof-of-concept, we show how such structures can be converted to metallic features *via* thermolysis and subsequent electroless deposition.

RESULTS AND DISCUSSION

For these experiments, Pd alkanethiolates are an ideal choice of ink since they are soluble in a wide variety of

organic solvents including toluene, chloroform, and acetone.²⁷ The low solubility of Pd alkanethiolates in water may hinder the transfer from the tip to the surface through the water meniscus,²⁸ which is the conventional transfer medium for DPN. Pd alkanethiolates, however, are metallomesogens²⁹ (liquid crystals that contain metals) and thus should remain liquid on the tip of an AFM and transfer *via* liquid ink mechanisms.³⁰

Prior to evaluating the properties of Pd alkanethiolates as DPN inks, we characterized thin films formed by drop-casting a solution of Pd octylthiolate (in toluene) on a Si substrate. Upon evaporation of toluene under ambient conditions, the Pd octylthiolate ink appeared liquid-like and sticky. An X-ray diffraction (XRD) pattern of the film showed a series of periodic peaks (Figure S1 in the Supporting Information), and from these data, the period of the lamellae was estimated to be 24.8 Å according to the $d(001)$ reflection. Previous work on the lamellar structure of this molecule has shown that the lamellae are composed of two layers of alkanethiols, juxtaposed in opposite directions^{24,31} with the palladium–sulfur repeating units forming a backbone in the middle of a lamellar layer. Here, the orientation of the lamellae when deposited on a surface was probed by grazing incidence small-angle X-ray scattering (GISAXS).³² The GISAXS pattern shows high intensity in the vertical direction (Figure S2), which indicates that the Pd octylthiolate lamellae are standing upright on the surface.

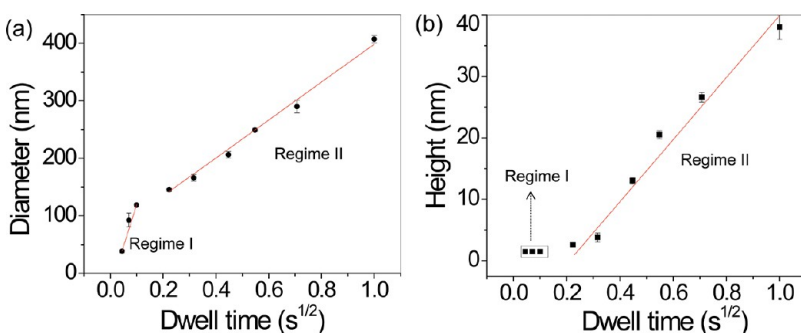


Figure 2. Variation of feature size with dwell time: (a) diameter and (b) height of the patterned Pd octylthiolate nanodots as a function of dwell time.

For DPN patterning, 1-D AFM tip arrays (12 tips) were coated with Pd octylthiolate ink (50 mM in toluene) using commercially available inkwells (Figure S3). After aligning the tips to inkwell microchannels, the tips were left in contact with the Pd octylthiolate ink for about \sim 30 s. Once the inked tip was brought into contact with a Si substrate under an ambient humidity of \sim 30% and temperature of \sim 20 °C, the liquid-like ink flowed continuously from the tip to the substrate, forming an array of patterned single Pd octylthiolate molecular layers (Figure 1a). The height of a Pd octylthiolate molecular layer measured by AFM is \sim 2.3 nm, which is in excellent agreement with the \sim 2.29 nm value estimated from molecular models and the XRD data on the thin film (2.4 ± 0.2 nm) (Figure 1a).²⁷ It should be noted that the structural motif of a single Pd octylthiolate molecular layer is a bilayer of hydrocarbon chains linked by Pd.²² Single molecular layers are formed relatively quickly (dwell time 0.01 s), and with increasing dwell time (0.05 s), two molecular layers are deposited (Figure 1b). Importantly, although the overall thickness (4.5 ± 0.3 nm) corresponds to the expected value for two layers, the thicknesses of the top and bottom layers are 2.9 ± 0.2 and 1.6 ± 0.1 nm, respectively. It is known in the literature that the topographic images of molecular layer-by-layer structures can show artifacts due to local variations in polarity¹⁹ and abrupt changes in topography³³ (as each step is only a molecular layer thick). When the molecular layers are deposited one on top of the other, the discrete entities may also have defects at the intercalation spots between the hydrocarbon chains (Scheme S1).^{27,34} Importantly, dwell time allows one to precisely control the deposition of subsequent layers, and therefore, increasing it to 0.1 s allowed us to form a third layer (Figure 1c). Phase images for the molecular multilayer structures (Figure S4) can be used to visualize the layers,³³ although quantitative analysis is difficult. The formation of these layered vertical stacks was unexpected and is quite interesting. We believe this occurs because the ink employed, Pd octylthiolate, is a covalent amphiphile³⁵ that can be driven to assemble into a single molecular layer at the water meniscus–air

interface. This is analogous to the Langmuir–Blodgett technique for monolayer formation, where the AFM tip acts here as both a point source for the molecular ink and driving force for the assembly. Here, the driving force for assembly arises from the movement of the tip and the meniscus as the tip traverses the surface. During the deposition process from AFM tip to substrate, there is a compromise reached between the natural tendency of the Pd octylthiolate toward stacked bilayer organization and the compatibility of such organization with the total volume and height/diameter aspect ratio of a particular deposited spot, which are determined by the deposition conditions such as dwell time and possibly the wetting properties of the substrate.¹⁸ After deposition of the molecule onto the surface, the inorganic backbone of Pd–S acts as a stabilizing influence and effectively cross-links the layer through Pd–Pd interactions.²⁷ Subsequent layers can be easily deposited on this relatively rigid layer.

A series of Pd octylthiolate dots were patterned on a Si substrate in order to systematically investigate the effect of dwell time on feature diameter and height (Figure 2). Interestingly, the variation in feature size showed two regimes. In the initial tip–substrate contact period (regime I, from dwell time = 0.01 to 0.05 s), the diameter of the patterned dot gradually increased while the height remained constant. In regime II (dwell time >0.05 s), both the diameter and height of the patterned dots increased linearly with the square root of time, indicating that the ink diffuses in the same manner as “traditional” molecular inks for DPN, such as mercaptohexadecanoic acid (MHA) and octadecanethiol (ODT).^{36,37} Unlike the covalent bond formation that occurs with a Au substrate in the case of MHA or ODT, here the ink transport mechanism is substrate-independent as there is no bonding between the Pd octylthiolate and the substrate. Indeed, patterning was feasible on a variety of substrates such as Si, Si/SiO₂, hexamethyldisilazane-coated hydrophobic Si, and polyimide (data not shown). These results demonstrate that, despite differing transport mechanisms between Pd octylthiolate and MHA, dwell time can be used to control the diameter and height of the patterned features.

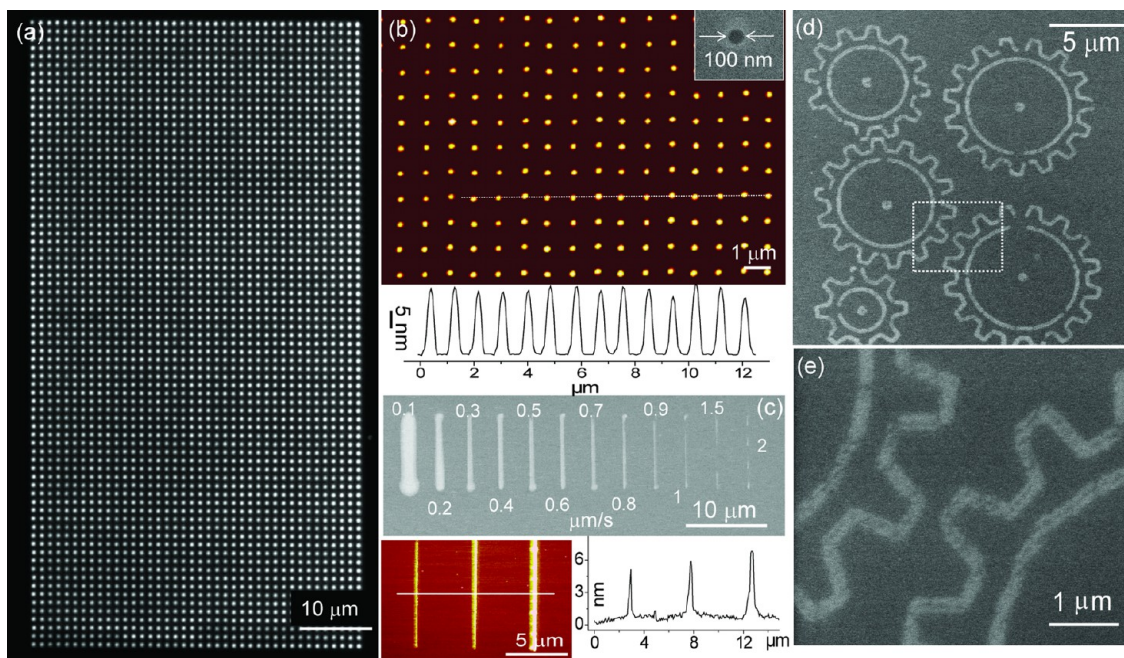


Figure 3. Versatile patterning of Pd octylthiolate by DPN. (a) Dark-field optical micrograph of an array of Pd octylthiolate dots over a large area. (b) AFM topography image and line profile of an array of patterned Pd thiolate dots. SEM image of a dot is shown in the inset. (c) SEM image of a series of lines with an increasing writing speed. AFM topography image and z-profile of the lines are shown below. The writing speed of the lines (ranging from 0.1 to $2 \mu\text{m} \cdot \text{s}^{-1}$) is indicated correspondingly. (d) SEM image of patterned planetary gear set. (e) Magnified view of the dotted box region in (d).

Apart from dwell time, the number of Pd octylthiolate layers can also be controlled by the molecular ink concentration. With an ink concentration of 10 mM, only monolayers of Pd octylthiolate were obtained, even with dwell times of 1 s (Figure S5). As previously noted, at an ink concentration of 50 mM, monolayer or multilayer structures can be formed, depending upon dwell time. At a concentration of 100 mM or higher, the height of the patterned features is not always an integer multiplied by the thickness of a lamellar monolayer, which indicates that such structures are an ill-defined mound of adsorbate. Remarkably, even the features formed at the highest ink concentration show a high degree of homogeneity as evident in the dark-field optical micrographs (Figure 3a). The height and diameter of such features, as determined by AFM and SEM measurements, are $18.6 \pm 0.5 \text{ nm}$ (Figure 3b) and 100 nm (Figure 3b inset), respectively. Since Pd octylthiolate is a low molecular weight ink, continuous lines (Figure S6) can be made without considerable viscous drag by appropriately selecting the writing speed and the ink concentration (Figure 3c). At an ink concentration of 100 mM and writing speeds higher than $1 \mu\text{m} \cdot \text{s}^{-1}$, the lines became discontinuous (Figure 3c). In the case of lines, multilayer structures were observed at 100 mM concentration, with little control over the number of layers (Figure S7). However, if the ink concentration is lower (50 mM), line features with tight control over the number of layers can be made (Figure S8). With respect to lines, two layers of molecules can be deposited reproducibly, but three

(or more) layers of molecules show a mound of multilayers along the length of the line (Figure S7). Thus, with higher ink concentrations and higher writing speeds, the Pd octylthiolate molecules are not able to assemble into well-defined lamellae.

To evaluate the versatility of the Pd octylthiolate patterning technique, we explored the types of structures that could be made. In addition to dots and lines, any structure that can be digitally imported can be generated. As a proof-of-concept, patterns in the form of planetary gears were made on a Si substrate (Figure 3d,e). In addition, the technique works for related but higher throughput scanning probe methods such as polymer-pen lithography (PPL) (Figure S8).^{38,39} Unlike DPN, the force exerted on the PPL tip array ($\sim 15\,000$ polydimethylsiloxane tips with $80 \mu\text{m}$ separation) can also be used to control the patterned feature size (Figure S9).

Importantly, the Pd octylthiolate features can be rapidly transformed into metallic Pd by annealing at 250°C in air (Figure 4a).⁴⁰ Since the number of layers in these structures was small (typically 10–12 nm thick, which equates to 5–6 molecular layers), the number of Pd atoms (expected Pd content is 41 wt %)⁴¹ is insufficient to produce contiguous Pd structures. AFM profile analysis after annealing shows that the average height of the Pd features is 2–4 nm, which is consistent with the loss of the organic material in the precursor structures (Figure S10). Pd nanoparticles are well-known catalysts for the electroless deposition of various metals such as Cu, Au, Ag, and Pd^{42,43} and conducting polymers

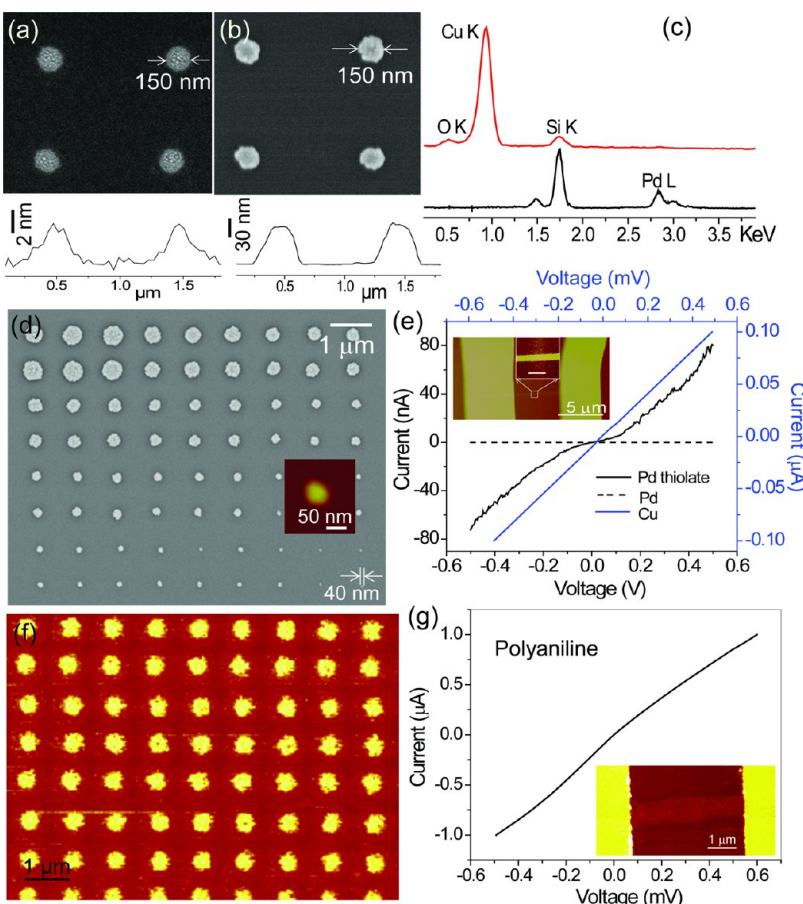


Figure 4. Thermolysis to Pd catalyst patterns for subsequent electroless deposition. SEM images of (a) as-thermolysed Pd dots and (b) after electroless deposition of Cu on Pd dots. AFM topographic line scan profiles are shown below, respectively. (c) EDS spectrum of thermolysed Pd dots (black) and the features after Cu electroless deposition on the Pd dots (red). (d) SEM image of an array of electroless deposited Cu features on thermolysed Pd dots with various sizes. (e) $I-V$ characteristics of Pd octylthiolate line patterned between electrodes (solid black line), after thermolysis (dashed black line), and after electroless Cu deposition (solid blue line). (f) AFM image of PANI deposited on Pd dots. (g) $I-V$ characteristics of a patterned PANI line. Inset shows the AFM image of the measured PANI line.

such as polyaniline (PANI).⁴⁴ Therefore, these structures can, in principle, be used as templates to construct nanocircuitry. To evaluate the potential for doing so, we explored the electroless deposition of Cu onto Pd-generated dots and lines (Figure 4b). The electroless deposition was performed by dipping the patterned substrate into an alkaline solution of CuSO_4 complexed with sodium potassium tartrate for 30 s, followed by the addition of formaldehyde as a reducing agent.⁴² After electroless deposition, energy-dispersive X-ray spectra (EDS) from the patterned features showed the presence of both Cu and Pd (Figure 4c and XRD in Figure S11). The width of the Cu/Pd features did not vary noticeably (Figure S10), but the height increased to ~ 65 – 70 nm, which is more than a factor of 10 when compared to the original feature height. During the electroless deposition, after the first layer of Cu is deposited onto Pd, further Cu deposition occurs in an autocatalytic fashion. The electroless deposition is a spontaneous reaction, and the feature size (height as well as diameter) can be controlled with deposition time (Figure S12). Uniform deposition of Cu was obtained down to ~ 40 nm

diameter, which was the smallest patterned dot size of the Pd catalyst (Figure 4d and Figure S13). To estimate the correlation between the patterning parameters of Pd octylthiolate and the obtained Cu features, the volume of patterned Cu dots was calculated. The volume was found to increase linearly with square root of dwell time. Thus, dwell time during the patterning of Pd octylthiolate can be used to control the diameter as well as the height of the final Cu features (Figure S14).

Electrical characterization of patterned Pd lines was performed to determine the utility of Pd octylthiolate ink for writing conductive conduits. A line of Pd octylthiolate was written by DPN bridging two Au electrodes (on Si/SiO_2 substrate) that were predefined by photolithography (Figure 4e inset). Current–voltage characteristics of the as-written Pd octylthiolate line are nonlinear (Figure 4e), which is typical for this molecule.²¹ After thermolysis, there was no detectable current, which is attributed to the formation of discontinuous Pd nanoparticles (*vide supra*). After electroless Cu deposition, the current increased to a few microamps, indicating that the Cu line was continuous

(Figure S15). The resistivity of the Cu line was $\sim 20 \mu\Omega \cdot \text{cm}$, which is 10 times higher than the bulk Cu resistivity ($1.7 \mu\Omega \cdot \text{cm}$). The increased resistivity compared to that in the bulk could be due to interface scattering at grain boundaries within the Cu line.⁴⁵ Nevertheless, this process provides an easy way of making electrical contacts to nanomaterials. Alternatively, this method can be useful for defining gap electrodes (Figure S16). Importantly, this method surpasses DPN-induced deposition of nanoparticles for conductive traces⁴⁶ both in terms of achievable resolution and uniformity of the features.

Pd patterns can serve as catalysts for electroless deposition of both inorganic and organic materials. As a proof-of-concept, we also performed electroless deposition of PANI. Autocatalytic polymerization of aniline initiated by a Pd catalyst surface leads to electroless deposition of PANI on Pd (Figure 4f) as confirmed by IR spectroscopy (Figure S17). Current–voltage responses were measured from the conductive line trace of PANI (in a similar setup as that of Cu line described above) and are consistent with the literature

values,⁴⁷ confirming that PANI has been uniformly deposited on the Pd lines (Figure 4g).

CONCLUSION

This work is interesting for the following reasons: palladium octylthiolate represents a new liquid ink for DPN where the number of molecular layers and thickness and volume of a given feature can be precisely controlled during patterning. With this method, one can create molecular nanoreactors and guide the number of metal atoms in the resulting features. Therefore, these structures can be used for generating contiguous lines and circuits or, alternatively, novel catalysts. As such, the present method represents a parallel, high-throughput, and more controllable alternative to e-beam lithography for making metallic nanostructures.⁴⁸ Furthermore, this study suggests that the scope of the inks that can be used for DPN should be rapidly expanded to molecules which form lamellar supramolecular architectures and lead to interesting structures of potential importance in catalysis, electronics, and photonics.

METHODS

Materials. Palladium(II) acetate (98%), octanethiol, isopropyl alcohol, and toluene were purchased from Sigma-Aldrich and used without further purification. Palladium octylthiolate ($\text{Pd}(\text{SC}_8\text{H}_{17})_2$) was prepared as follows.⁴¹ Equimolar $\text{Pd}(\text{OAc})_2$ and octanethiol were mixed in a stirred solution of toluene. As the reaction proceeded, a color change from orange-yellow to deep red was observed. After 15 min of stirring, the Pd octylthiolate solution was washed with water. After vigorous shaking, the toluene and water separated into layers, with the organic layer containing Pd octylthiolate and the aqueous layer containing acetic acid, the main byproduct. From here, purified Pd octylthiolate was diluted in toluene to obtain the desired concentration. Si(100) wafers with native oxide, cleaned by sequential rinsing with acetone and isopropyl alcohol, were used for patterning.

DPN Patterning Process. All DPN patterning was performed with 1-D type-M tip arrays from Nanolnk in either a DPN5000 or an NScriptor (both from Nanolnk, Inc.). The tips can be inked by either dip-coating for 30 s or using type-M inkwells (Nanolnk, Inc.). In general, we noticed that inkwells gave more uniform loading of ink onto the tips than dip-coating. The patterning was done in ambient conditions with humidity of 35–50% and a temperature of 20 °C. Notably, while the humidity varied day-to-day, it did not significantly affect the patterned feature size. The 1-D cantilever tip arrays were aligned parallel to the substrate by optical leveling. The patterns were generated using InkCAD software (Nanolnk, Inc.), which allows one to control feature position and tip–substrate contact time.

PPL Patterning Process. Polymer pen tip arrays with $80 \mu\text{m}$ spacing between tips were prepared as previously reported.³⁸ Briefly, the pen arrays were made from hard PDMS (h-PDMS), which was stirred, degassed, and poured on top of the soft pen array master. Prior to curing, a precleaned glass slide (VWR, Inc.) was then placed on top of the elastomer array and the whole assembly was cured at 80 °C overnight. After curing, the polymer pen array was carefully separated from the pyramid master by using a razor blade. The ink solution of Pd octylthiolate (50 mM) was spin-coated onto the PDMS tip arrays (1 mL ink, 2000 rpm, 1 min). PPL was carried out on an XE-150 AFM with a customized PPL head (Park Systems), using custom XEP

software (Park Systems) at a relative humidity of $\sim 80\%$ and temperature of 25–29 °C. The leveling between the pen arrays and the sample was adjusted with an XY scanning tilting stage.

Thermolysis. After DPN or PPL, the patterned Pd octylthiolate samples were thermolized on a hot plate set to a temperature of 250 °C in ambient atmosphere for 1 h.

Electroless Deposition. The copper plating bath used for electroless Cu deposition⁴² consisted of solution A (1.5 g of CuSO_4 , 7 g of sodium potassium tartrate, and 7 g of NaOH in 50 mL of water) and solution B (37.2 wt % aqueous formaldehyde solution). The glass substrate patterned with Pd dots was immersed in solution A, while solution B (10:1 ratio of A/B, v/v) was added directly onto the patterned face. The stock solution of A gave better results when used within a week.

For PANI deposition, 5% aniline and 0.6 M H_2SO_4 were mixed in an equal ratio (v/v), and the patterned substrate or thin film was dipped inside the solution for ~ 2 h in air.⁴⁴ An acidic solution of aniline in sulfuric acid in the presence of oxygen leads to oxidation, resulting in PANI film deposition selectively onto Pd dots. The Pd thin film turned green after the deposition of PANI.

Characterization. XRD on thin films of Pd octylthiolate, Pd, and Cu/Pd was performed by a Rigaku ATX-G. All grazing incident small-angle X-ray scattering (GISAXS) experiments were conducted at the Basic Research Sciences Synchrotron Radiation Center (BESSRC) at the Advanced Photon Source (APS) located at Argonne National Laboratory. The samples were probed using 12 keV (1.33 Å) X-rays, and scattering was calibrated from a silver behenate standard. The beam was collimated using two sets of slits. A pinhole was used to remove parasitic scattering. The beam width was approximately 200–300 μm in diameter. Fourier transform infrared spectroscopy (FTIR, Thermo Nicolet, Nexus 870) on PANI was done by scraping a small amount of the film and pelletizing it with KBr. I – V measurements were performed under ambient conditions using a Keithley 4200 semiconductor characterization system. The samples were examined using a Hitachi S-8030 SEM at an acceleration voltage of 5 kV and a current of 20 μA , with the probe current set to normal and focus mode set to ultrahigh resolution. Only the upper second electron detector was used. AFM was performed using a Bruker Dimension Icon in tapping mode,

using a PPP-NCH tip (Nanosensors). AFM data analysis was performed using Nanoscope software.

Conflict of Interest: The authors declare no competing financial interest.

Acknowledgment. This material is based upon work supported DARPA/MTO Award N66001-08-1-2044, AOARD Award FA2386-10-1-4065, AFOSR Awards FA9550-12-1-0280 and FA9550-12-1-0141, NSF Awards DBI-1152139 and DMB-1124131, DOD/NPS/NSSEF Fellowship Awards N00244-09-1-0012 and N00244-09-1-0071, Chicago Biomedical Consortium with support from Searle Funds at The Chicago Community Trust. Any opinions, findings, and conclusions or recommendations expressed in this publication are those of the authors and do not necessarily reflect the views of the sponsors. B.R. acknowledges the Indo-US Science & Technology Forum (IUSSTF) for a visiting fellowship. D.J.E. acknowledges the DOD and AFOSR for a National Defense Science and Engineering Graduate (NDSEG) fellowship, 32 CFR 168a. B.R. thanks A.J. Sensei for help in GISAXS analysis. The authors thank the Northwestern University Electron Probe Instrumentation Center (EPIC).

Supporting Information Available: XRD and GISAXS data of Pd octylthiolate thin film; optical images of the inkwell with Pd octylthiolate ink; AFM images of lines and dots made by DPN and PPL; SEM, AFM, XRD, and I-V of electroless Cu; FTIR of PANI. This material is available free of charge via the Internet at <http://pubs.acs.org>.

REFERENCES AND NOTES

- Piner, R. D.; Zhu, J.; Xu, F.; Hong, S.; Mirkin, C. A. Dip-Pen Nanolithography. *Science* **1999**, *283*, 661–663.
- Salaita, K.; Wang, Y.; Fragala, J.; Vega, R. A.; Liu, C.; Mirkin, C. A. Massively Parallel Dip-Pen Nanolithography with 55000-Pen Two-Dimensional Arrays. *Angew. Chem., Int. Ed.* **2006**, *45*, 7220–7223.
- Salaita, K.; Wang, Y.; Mirkin, C. A. Applications of Dip-Pen Nanolithography. *Nat. Nanotechnol.* **2007**, *2*, 145–155.
- Ginger, D. S.; Zhang, H.; Mirkin, C. A. The Evolution of Dip-Pen Nanolithography. *Angew. Chem., Int. Ed.* **2004**, *43*, 30–45.
- Chai, J.; Huo, F.; Zheng, Z.; Giam, L. R.; Shim, W.; Mirkin, C. A. Scanning Probe Block Copolymer Lithography. *Proc. Natl. Acad. Sci. U.S.A.* **2010**, *107*, 20202–20206.
- Senesi, A. J.; Rozkiewicz, D. I.; Reinhoudt, D. N.; Mirkin, C. A. Agarose-Assisted Dip-Pen Nanolithography of Oligonucleotides and Proteins. *ACS Nano* **2009**, *3*, 2394–2402.
- Ivanisevic, A.; Mirkin, C. A. Dip-Pen Nanolithography on Semiconductor Surfaces. *J. Am. Chem. Soc.* **2001**, *123*, 7887–7889.
- Porter, L. A.; Choi, H. C.; Schmeltzer, J. M.; Ribbe, A. E.; Elliott, L. C. C.; Buriak, J. M. Electroless Nanoparticle Film Deposition Compatible with Photolithography, Microcontact Printing, and Dip-Pen Nanolithography Patterning Technologies. *Nano Lett.* **2002**, *2*, 1369–1372.
- Wang, W. M.; Stoltenberg, R. M.; Liu, S.; Bao, Z. Direct Patterning of Gold Nanoparticles Using Dip-Pen Nanolithography. *ACS Nano* **2008**, *2*, 2135–2142.
- Su, M.; Liu, X.; Li, S.-Y.; Dravid, V. P.; Mirkin, C. A. Moving beyond Molecules: Patterning Solid-State Features via Dip-Pen Nanolithography with Sol-Based Inks. *J. Am. Chem. Soc.* **2002**, *124*, 1560–1561.
- Wilson, D. L.; Martin, R.; Hong, S.; Cronin-Golomb, M.; Mirkin, C. A.; Kaplan, D. L. Surface Organization and Nanopatterning of Collagen by Dip-Pen Nanolithography. *Proc. Natl. Acad. Sci. U.S.A.* **2001**, *98*, 13660–13664.
- Lenhert, S.; Sun, P.; Wang, Y.; Fuchs, H.; Mirkin, C. A. Massively Parallel Dip-Pen Nanolithography of Heterogeneous Supported Phospholipid Multilayer Patterns. *Small* **2007**, *3*, 71–75.
- Byrd, H.; Pike, J. K.; Talham, D. R. Inorganic Monolayers Formed at an Organic Template: A Langmuir–Blodgett Route to Monolayer and Multilayer Films of Zirconium Octadecylphosphonate. *Chem. Mater.* **1993**, *5*, 709–715.
- Ploog, K. Molecular Beam Epitaxy of III–V Compounds: Application of MBE-Grown Films. *Annu. Rev. Mater. Sci.* **1982**, *12*, 123–148.
- Levchenko, A. A.; Yee, C. K.; Parikh, A. N.; Navrotsky, A. Energetics of Self-Assembly and Chain Confinement in Silver Alkanethiolates: Enthalpy–Entropy Interplay. *Chem. Mater.* **2005**, *17*, 5428–5438.
- Roberts, G. G. Molecular Electronics Using Langmuir–Blodgett Films. *Electronic and Photonic Applications of Polymers*; American Chemical Society: Washington, DC, 1988; Vol. 218, pp 225–270.
- Lenhert, S.; Zhang, L.; Mueller, J.; Wiesmann, H. P.; Erker, G.; Fuchs, H.; Chi, L. Self-Organized Complex Patterning: Langmuir–Blodgett Lithography. *Adv. Mater.* **2004**, *16*, 619–624.
- Maoz, R.; Frydman, E.; Cohen, S. R.; Sagiv, J. “Constructive Nanolithography”: Inert Monolayers as Patternable Templates for *In-Situ* Nanofabrication of Metal–Semiconductor–Organic Surface Structures—A Generic Approach. *Adv. Mater.* **2000**, *12*, 725–731.
- Zeira, A.; Chowdhury, D.; Hoeppener, S.; Liu, S.; Berson, J.; Cohen, S. R.; Maoz, R.; Sagiv, J. Patterned Organosilane Monolayers as Lyophobic–Lyophilic Guiding Templates in Surface Self-Assembly: Monolayer Self-Assembly versus Wetting-Driven Self-Assembly. *Langmuir* **2009**, *25*, 13984–14001.
- Chowdhury, D.; Maoz, R.; Sagiv, J. Wetting Driven Self-Assembly as a New Approach to Template-Guided Fabrication of Metal Nanopatterns. *Nano Lett.* **2007**, *7*, 1770–1778.
- John, N. S.; Pati, S. K.; Kulkarni, G. U. Electrical Characteristics of Layered Palladium Alkanethiolates by Conducting Atomic Force Microscopy. *Appl. Phys. Lett.* **2008**, *92*, 013120–013123.
- John, N. S.; Kulkarni, G. U.; Datta, A.; Pati, S. K.; Komori, F.; Kavitha, G.; Narayana, C.; Sanyal, M. K. Magnetic Interactions in Layered Nickel Alkanethiolates. *J. Phys. Chem. C* **2007**, *111*, 1868–1870.
- Zhang, Y. X.; Zeng, H. C. Gold(I)-Alkanethiolate Nanotubes. *Adv. Mater.* **2009**, *21*, 4962–4965.
- Hu, L.; de la Rama, L. P.; Efremov, M. Y.; Anahory, Y.; Schiettekatte, F.; Allen, L. H. Synthesis and Characterization of Single-Layer Silver–Decanethiolate Lamellar Crystals. *J. Am. Chem. Soc.* **2011**, *133*, 4367–4376.
- Sandhyaran, N.; Pradeep, T. An Investigation of the Structure and Properties of Layered Copper Thiolates. *J. Mater. Chem.* **2001**, *11*, 1294–1299.
- Bhuvana, T.; Kulkarni, G. U. Highly Conducting Patterned Pd Nanowires by Direct-Write Electron Beam Lithography. *ACS Nano* **2008**, *2*, 457–462.
- John, N. S.; Thomas, P. J.; Kulkarni, G. U. Self-Assembled Hybrid Bilayers of Palladium Alkanethiolates. *J. Phys. Chem. B* **2003**, *107*, 11376–11381.
- Cho, N.; Ryu, S.; Kim, B.; Schatz, G. C.; Hong, S. Phase of Molecular Ink in Nanoscale Direct Deposition Processes. *J. Chem. Phys.* **2006**, *124*, 024714–024716.
- Baena, M. J.; Espinet, P.; Lequerica, M. C.; Levelut, A. M. Mesogenic Behavior of Silver Thiolates with Layered Structure in the Solid State: Covalent Soaps. *J. Am. Chem. Soc.* **1992**, *114*, 4182–4185.
- Nakashima, H.; Higgins, M. J.; O’Connell, C.; Torimitsu, K.; Wallace, G. G. Liquid Deposition Patterning of Conducting Polymer Ink onto Hard and Soft Flexible Substrates via Dip-Pen Nanolithography. *Langmuir* **2011**, *28*, 804–811.
- Dance, I. G.; Fisher, K. J.; Banda, R. M. H.; Scudder, M. L. Layered Structure of Crystalline Compounds AgSR. *Inorg. Chem.* **1991**, *30*, 183–187.
- Herman, D. J.; Goldberger, J. E.; Chao, S.; Martin, D. T.; Stupp, S. I. Orienting Periodic Organic–Inorganic Nanoscale Domains through One-Step Electrodeposition. *ACS Nano* **2010**, *5*, 565–573.
- Garcia, R.; Perez, R. Dynamic Atomic Force Microscopy Methods. *Surf. Sci. Rep.* **2002**, *47*, 197–301.
- Cha, S.-H.; Kim, K.-H.; Lee, W.-K.; Lee, J. C. Highly Ordered Bilayer Structures of Gold(I)–Alkanethiolates Having Two Types of Alkyl Groups. *J. Ind. Eng. Chem.* **2010**, *16*, 816–822.
- Thomas, P. J.; Lavanya, A.; Sabareesh, V.; Kulkarni, G. U. Self-Assembling Bilayers of Palladiumthiolates in Organic Media. *Proc. Indian Acad. Sci.* **2001**, *113*, 611–619.

36. Rozhok, S.; Piner, R.; Mirkin, C. A. Dip-Pen Nanolithography: What Controls Ink Transport? *J. Phys. Chem. B* **2003**, *107*, 751–757.
37. Jang, J.; Hong, S.; Schatz, G. C.; Ratner, M. A. Self-Assembly of Ink Molecules in Dip-Pen Nanolithography: A Diffusion Model. *J. Chem. Phys.* **2001**, *115*, 2721–2729.
38. Huo, F.; Zheng, Z.; Zheng, G.; Giam, L. R.; Zhang, H.; Mirkin, C. A. Polymer Pen Lithography. *Science* **2008**, *321*, 1658–1660.
39. Giam, L. R.; Mirkin, C. A. Cantilever-Free Scanning Probe Molecular Printing. *Angew. Chem., Int. Ed.* **2011**, *50*, 7482–7485.
40. Carotenuto, G.; Martorana, B.; Perlo, P.; Nicolais, L. A Universal Method for the Synthesis of Metal and Metal Sulfide Clusters Embedded in Polymer Matrices. *J. Mater. Chem.* **2003**, *13*, 2927–2930.
41. Radha, B.; Kulkarni, G. U. A Modified Micromolding Method for Sub-100-nm Direct Patterning of Pd Nanowires. *Small* **2009**, *5*, 2271–2275.
42. Hidber, P. C.; Helbig, W.; Kim, E.; Whitesides, G. M. Micro-contact Printing of Palladium Colloids: Micron-Scale Patterning by Electroless Deposition of Copper. *Langmuir* **1996**, *12*, 1375–1380.
43. Tan, Y.; Gu, J.; Zang, X.; Xu, W.; Shi, K.; Xu, L.; Zhang, D. Versatile Fabrication of Intact Three-Dimensional Metallic Butterfly Wing Scales with Hierarchical Sub-micrometer Structures. *Angew. Chem., Int. Ed.* **2011**, *50*, 8307–8311.
44. Liao, C.; Gu, M. Electroless Deposition of Polyaniline Film via Autocatalytic Polymerization of Aniline. *Thin Solid Films* **2002**, *408*, 37–42.
45. Hsu, Y.; Standaert, T.; Oehrlein, G. S.; Kuan, T. S.; Sayre, E.; Rose, K.; Lee, K. Y.; Rossnagel, S. M. Fabrication of Cu Interconnects of 50 nm Linewidth by Electron-Beam Lithography and High-Density Plasma Etching. *J. Vac. Sci. Technol., B* **1998**, *16*, 3344–3348.
46. Wang, H.-T.; Nafday, O. A.; Haaheim, J. R.; Tevaarwerk, E.; Amro, N. A.; Sanedrin, R. G.; Chang, C.-Y.; Ren, F.; Pearton, S. J. Toward Conductive Traces: Dip Pen Nanolithography of Silver Nanoparticle-Based Inks. *Appl. Phys. Lett.* **2008**, *93*, 143105–143107.
47. Wu, C.-G.; Chang, S. S. Nanoscale Measurements of Conducting Domains and Current–Voltage Characteristics of Chemically Deposited Polyaniline Films. *J. Phys. Chem. B* **2005**, *109*, 825–832.
48. Wang, W. M.; LeMieux, M. C.; Selvarasah, S.; Dokmeci, M. R.; Bao, Z. Dip-Pen Nanolithography of Electrical Contacts to Single-Walled Carbon Nanotubes. *ACS Nano* **2009**, *3*, 3543–3551.